BIOCHEMISTRY
including biophysical chemistry & molecular biology
Article

Biochemistry **2010,** *49,* 9353–9360 9353
DOI: 10.1021/bi1012657

Myo1e Binds Anionic Phospholipids with High Affinity†

Elizabeth A. Feeser,‡ Cherry Mae G. Ignacio,§ Mira Krendel,∥ and E. Michael Ostap*,‡

‡*Pennsylvania Muscle Institute and Department of Physiology, University of Pennsylvania School of Medicine, Philadelphia, Pennsylvania 19104,* §*Department of Biochemistry and Molecular Biology, and* ∥*Department of Cell and Developmental Biology, SUNY Upstate Medical University, Syracuse, New York 13210*

Received August 6, 2010; Revised Manuscript Received September 16, 2010

ABSTRACT: Myo1e is a single-headed motor protein that has been shown to play roles in clathrin-mediated endocytosis in HeLa cells and podocyte function in the kidney. The myo1e C-terminal tail domain includes a basic region that is required for localization to clathrin-coated vesicles and contains a putative pleckstrin-homology (PH) domain that has been shown to play a role in phospholipid binding in other myosin-I proteins. We used sedimentation assays, stopped-flow fluorescence, and fluorescence microscopy to determine the membrane binding affinities, kinetics, and *in vivo* localization of fluorescently labeled recombinant myo1e-tail constructs. We found that the myo1e tail binds tightly to large unilamellar vesicles (LUVs) containing physiological concentrations of the anionic phospholipids phosphatidylinositol 4,5-bisphosphate (PtdIns(4,5)P_2) or phosphatidylserine. The rate of myo1e attachment to LUVs nears the diffusion limit while the calculated rate of detachment from LUVs is slow ($k_{diss} \leq 0.4\ s^{-1}$). Mutation of conserved residues in the myo1e PH domain has little effect on lipid binding *in vitro* or membrane localization *in vivo*. Soluble inositol phosphate headgroups, such as inositol 1,4,5-trisphosphate, can compete with PtdIns(4,5)P_2 for binding, but the apparent affinity for the soluble inositol phosphate is substantially lower than that for PtdIns(4,5)P_2. These results suggest that myo1e binds lipids through nonspecific electrostatic interactions rather than a stereospecific protein−phosphoinositide interaction.

Myosin-I family members are actin-based molecular motors that play roles in membrane dynamics and membrane trafficking. Myosin-Is link cellular membranes to the actin cytoskeleton, as myosin-I isoforms can move actin relative to planar lipid membranes (*1*) and modulate membrane tension *in vivo* (*2*). All myosin-I isoforms, including eight isoforms in vertebrates (myo1a−h), have three common domains: a motor domain that binds actin and hydrolyzes ATP, a regulatory domain that binds calmodulin or other myosin light chains, and a tail domain that interacts with membranes and tail-binding proteins. Myosin-Is are broadly classified as short-tailed and long-tailed, where the tail domains of both classes have a positively charged tail-homology-1 (TH1)[1] region (*3*) and the long-tailed isoforms also contain proline-rich (PRD) and Src-homology-3 (SH3) domains.

Several myosin-I isoforms have been shown to interact directly with membranes (*4*−*8*) via electrostatic interactions between the TH1 region and anionic phospholipids. We recently discovered that a PH domain resides within the TH1 regions of all myosin-I isoforms and that vertebrate myo1c (a short-tailed isoform) interacts with physiological concentrations of phosphoinositides via this domain (*9*). Point mutations of residues known to be essential for polyphosphoinositide binding in previously characterized PH domains inhibit myo1c binding to phosphoinositides *in vitro*. Increasing levels of negatively charged lipids further increases affinity of myo1c for membranes, suggesting electrostatic interactions outside of the canonical PH regions contribute to membrane binding, similar to some other PH domain containing proteins (*10*, *11*).

PH domains appear to be present in all myosin-I isoforms, and point mutations in PH domains disrupt *in vivo* membrane binding of vertebrate myo1c, myo1f, myo1g, and myo1b (*9*, *12*−*14*). Although conserved PH domain residues are required for myo1g membrane localization, the PH domain alone is not sufficient for localization (*12*). *Acanthamoeba* myosin-IC, a long-tailed isoform that lacks one of the PH domain consensus residues, binds membranes both *in vitro* and *in vivo*, and mutation of a conserved PH domain residue does not dramatically affect membrane binding (*8*). Together, these data suggest that myosin-Is interact with membrane lipids through both a specific interaction mediated by the PH domain and by nonspecific electrostatic interactions mediated by basic residues in other regions of the tail domain (see Figure 1).

Myo1e is a widely expressed vertebrate long-tailed myosin-I isoform (previously known as myr-3 or human myosin-IC) that localizes to phagocytic cups (*15*), adherens-type intercellular junctions (*16*), and clathrin-containing puncta (*17*). Expression of a dominant-negative myo1e construct in human cell lines inhibits endocytosis (*17*), and genetic removal of the protein causes kidney disease in mice (*18*). Myo1e has been shown to interact with proteins involved in endocytosis and actin dynamics, including dynamin, synaptojanin (*17*), and CARMIL-1a/Acan125 (*19*, *20*), presumably via the myo1e SH3 domain. In localization studies,

†This work was supported by a NIH/NRSA fellowship to E.A.F. (GM090551), a NephCure Foundation Young Investigator Grant to M. K., and a grant from the NIH to E.M.O. (GM057247).

*Address correspondence to this author. E-mail: ostap@mail.med.upenn.edu. Phone: 215-573-9758. Fax: 215-573-2273.

[1]Abbreviations: DOPC, 1,2-dioleoyl-*sn*-glycero-3-phosphocholine; DOPS, 1,2-dioleoyl-*sn*-glycero-3-phospho-L-serine; PtdIns(4,5)P_2, L-α-phosphatidylinositol 4,5-bisphosphate; 18:1 PtdIns(3,5)P_2, 1,2-dioleoyl-*sn*-glycero-3-phospho-(1′-*myo*-inositol 3′,5′-bisphosphate); 18:1 PtdIns(4,5)P_2, 1,2-dioleoyl-*sn*-glycero-3-phospho-(1′-*myo*-inositol 3′,5′-bisphosphate); 18:1 PtdIns(3,4,5)P_3, 1,2-dioleoyl-*sn*-glycero-3-phospho-(1′-*myo*-inositol 3′,4′,5′-trisphosphate); $InsP_3$, D-*myo*-inositol 1,4,5-triphosphate; $InsP_6$, *myo*-inositol hexakisphosphate; PH domain, pleckstrin-homology domain; LUV, large unilamellar vesicle; TH1, tail-homology-1; PRD, proline-rich domain; SH3, Src-homology-3; GFP, green fluorescent protein; GST, glutathione *S*-transferase; DMEM, Dulbecco's modified Eagle medium; FBS, fetal bovine serum.

Published on Web 09/22/2010

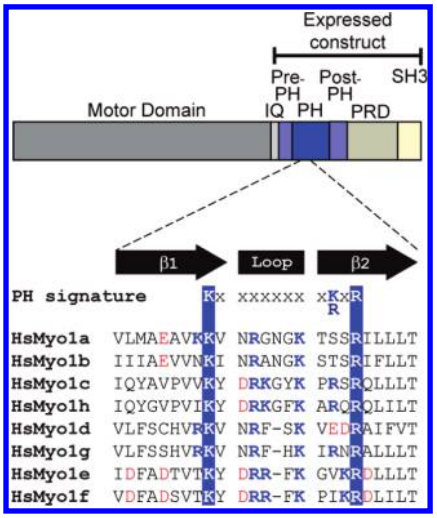

FIGURE 1: Myo1e schematic and PH domain sequence alignment. The expressed myo1e construct (top) includes the entire myo1e tail with an N-terminal GFP-His tag. Domains span the following residues: motor, 20−691; IQ, 692−717; pre-PH, 718−762; PH, 763−864; post-PH, 865−923; PRD, 924−1055; SH3, 1056−1107. Alignment of the PH domain signature motif of human myosin-1 isoforms (Bottom) shows conservation of conserved lysine and arginine residues. The order in which the isoforms are listed clusters proteins with greatest sequence similarity. Residues mutated in these studies are indicated with a blue box. For other residues, blue indicates basic residues, and red indicates acidic residues.

myo1e appears to associate with membranes. However, the membrane binding properties of myo1e have not been explored.

In this study, we characterized the interaction of myo1e with anionic phospholipids. We report the effective affinity constants, as well as the rate constants for association and dissociation, for myo1e binding to vesicles of various lipid composition. Our data show that myo1e binds tightly to vesicles containing physiological concentrations of either phosphatidylserine or phosphoinositides. Binding studies with constructs that contain PH domain point mutations indicate that conserved PH domain residues only moderately affect *in vitro* membrane binding and do not affect *in vivo* membrane localization. These findings (a) suggest that myo1e binds tightly to physiological concentrations of acidic phospholipids that are not necessarily phosphoinositides and (b) show that there is substantial diversity in the binding of the various myosin-I isoforms to membranes.

EXPERIMENTAL PROCEDURES

Buffers and Reagents. All experiments were performed in HNa100 buffer containing 10 mM HEPES, pH 7.0, 100 mM NaCl, 1 mM EGTA, and 1 mM DTT. $MgCl_2$ was added at a final concentration of 1 mM where indicated. All experiments were performed in the presence of 1 μM calmodulin. The following lipids were from Avanti: 1,2-dioleoyl-*sn*-glycero-3-phosphocholine (DOPC); 1,2-dioleoyl-*sn*-glycero-3-phospho-L-serine (DOPS), L-α-phosphatidylinositol 4,5-bisphosphate [PtdIns(4,5)P_2], 1,2-dioleoyl-*sn*-glycero-3-phospho-(1′-*myo*-inositol 3′,5′-bisphosphate) [18:1 PtdIns(3,5)P_2], 1,2-dioleoyl-*sn*-glycero-3-phospho-(1′-*myo*-inositol 3′,5′-bisphosphate) [18:1 PtdIns(4,5)P_2], and 1,2-dioleoyl-*sn*-glycero-3-phospho-(1′-*myo*-inositol 3′,4′,5′-trisphosphate) [18:1 PtdIns(3,4,5)P_3]. D-*myo*-Inositol 1,4,5-triphosphate ($InsP_3$) was from Cayman Chemical, and *myo*-inositol hexakisphosphate ($InsP_6$) and ATP were from Sigma.

Generation of Wild-Type and Mutant Expression Constructs. PCR was used to insert hexahistidine-encoding bases into the previously described pEGFP-C1-myo1e-tail construct (*17*). The final construct includes residues 710−1108 of human myo1e (myo1e tail) with N-terminal hexahistidine and green fluorescent protein (GFP) tags. Bases encoding the His_6-GFP-myo1e-tail construct were PCR amplified and cloned into the pBlueBac4.5 baculovirus transfer vector (Invitrogen).

PH domain mutants were generated using the QuickChange II mutagenesis kit (Stratagene) with the pBlueBac4.5 plasmid according to manufacturer's instructions. The K772A mutant was generated using primers 5′-tttcgcagacacagtcaccgcgtatgacag-gaggttcaag-3′ and 5′-cttgaacctcctgtcatacgcggtgactgtgtctgcgaaa-3′. The R882A mutant was generated using primers 5′-ggaggtt-caagggtgtaaaggcagacctgctcctta-3′ and 5′-taaggagcaggtctgcctttta-caccctgaacctcc-3′.

Recombinant baculovirus was generated from pBlueBac4.5 plasmid using standard procedures.

Protein Expression and Purification. Wild-type and mutant His_6-GFP-myo1e tail was coexpressed with calmodulin in Sf9 cells. Cells were harvested by centrifugation and stored at −80 °C. Cells were resuspended in buffer containing 50 mM sodium phosphate, pH 7.4, 0.5 M NaCl, 0.5 mM EGTA, 1 μM DTT, 20 mM imidazole, 0.5% igepal, 0.01 mg/mL aprotinin, 0.01 mg/mL leupeptin, and 1 mM phenylmethanesulfonyl fluoride and lysed with five strokes in a Dounce homogenizer. Cell lysate was cleared by centrifugation at 100000*g* for 1 h. The supernatant was sonicated with six 15 s pulses, incubated with 10 μg/mL RNase A (Roche) and 5 μg/mL DNase I (Roche), and loaded on a Ni-NTA (Qiagen) column. The column was washed in 8 column volumes of the resuspension buffer without igepal. His_6-GFP-myo1e tail was eluted in 10 mL of buffer containing 50 mM sodium phosphate, pH 7.4, 150 mM NaCl, 0.5 mM EGTA, 1 mM BME, and 150 mM imidazole plus 5 μM calmodulin. The eluant was diluted to 30 mL in buffer containing 50 mM HEPES, pH 7.4, 50 mM NaCl, 1 mM EGTA, and 1 mM DTT and loaded on a MonoS column (GE Healthcare). His_6-GFP-myo1e tail was separated from contaminating proteins with a gradient of 0.1−1 M NaCl with His_6-GFP-myo1e tail eluting around 0.5 M NaCl. Because concentrated GFP-myo1e tail precipitates at low concentrations of NaCl, fractions containing the protein of interest were combined and stored in elution buffer. GFP-myo1e-tail concentrations were calculated from the absorbance of the protein sample at 488 nm using an extinction coefficient of 55000 M^{-1} cm^{-1}.

Glutathione *S*-transferase (GST) was expressed in *Escherichia coli* cells using the pGEX vector and purified by affinity chromatography with glutathione Sepharose 4B resin (GE Healthcare) according to manufacturer's instructions.

Recombinant chicken calmodulin was expressed and purified as described (*21*) and then further purified by anion-exchange chromatography on a MonoQ column (GE Healthcare).

Preparation of LUVs. Protocols for making LUVs with varying lipid content have been published (*7*). Chloroform-solvated lipids in the appropriate molar fractions were mixed and dried under nitrogen. Lipids for sedimentation assays were resuspended in a solution of 12 mM HEPES, pH 7.0, and 176 mM sucrose, while those for stopped-flow assays were resuspended in HNa100. Resuspended lipids were subjected to five freeze−thaw cycles, bath-sonicated for 1 min, and then extruded through 100 nm filters to generate vesicles of the desired size. Lipids for sedimentation assays were dialyzed overnight against HNa100. All LUVs were stored under nitrogen at 4 °C for no longer than 3 days.

Sedimentation Assays. Binding of GFP-myo1e tail to LUVs was determined by sedimentation assays similar to those described previously (*9*). Briefly, 200 μL samples containing 40 nM GFP-myo1e tail and sucrose-loaded LUVs were sedimented at 150000*g* for 30 min at 25 °C. GST at a final concentration of 0.25 mg/mL was included in all sedimentation assays to prevent nonspecific binding of GFP-myo1e tail to the centrifuge tubes. The top 160 μL of each sample was removed and assayed for GFP fluorescence in a fluorometer (PTI). The binding affinity of GFP-myo1e tail for LUVs is reported as an effective dissociation constant in terms of total lipid concentration (K_{eff}^{lipid}), which is the inverse of the partition coefficient (*22*). Binding data were fit to a hyperbola using KaleidaGraph (Synergy Software).

Stopped-Flow Assays. All measurements were performed at 22 °C in a stopped-flow instrument (Applied Photophysics). Fluorescence quenching measurements were performed in an L-format with an excitation wavelength of 488 nm and a 515 nm long-pass emission filter. Light scattering measurements were performed in an L-format with an excitation wavelength of 560 nm and a 515 nm long-pass emission filter.

Stopped-flow data were processed by averaging two to four individual traces from a single experiment and fitting this average to a two-exponential function [$y = A_{fast}(e^{-k_{fast}t}) + A_{slow}(e^{-k_{slow}t})$]; some traces showed no slow component and were fit to a single-exponential function [$y = A_{fast}(e^{-k_{fast}t})$]. A small decrease in fluorescence amplitude was observed upon mixing of the protein solution and buffer in the absence of lipid, so the amplitude of this blank sample was subtracted from the total amplitude ($A_{fast} + A_{slow}$) for each averaged trace. Corrected amplitudes were used to calculate fraction bound, and effective dissociation constants were determined using the same fitting methods described for sedimentation assays. Reported rates for each lipid concentration are the average of two to six experiments. An apparent second-order association rate constant (k_a) was determined from the slope of a linear fit to a plot of the average k_{fast} values versus total lipid concentration.

Inositol Phosphate Competition Experiments. Inositol phosphate binding to GFP-myo1e tail was measured by stopped-flow competition experiments with PtdIns(4,5)P_2 LUVs. Inositol phosphate was rapidly mixed with a preequilibrated solution of GFP-myo1e tail and LUVs. The average trace from each experiment was fit to a one- or two-exponential function. Some dissociation curves also had a slowly decreasing linear component that could also be observed upon mixing of GFP-myo1e tail with inositol phosphates in the absence of LUVs. When this fluorescence decrease was observed, transients were fit with a two-exponential function with an added linear component [$y = A_{fast}(e^{-k_{fast}t}) + A_{slow}(e^{-k_{slow}t}) + \text{slope} \times t$]. Fraction bound was determined from the total amplitude of the exponential components ($A_{fast} + A_{slow}$). Plots of fraction bound versus inositol phosphate concentration were fit as described (*9*). Rates varied significantly between experiments and are not reported. As a control, preequilibrated mixtures of GFP-myo1e tail and LUVs were rapidly mixed with 50 or 500 μM ATP.

In Vivo Localization Assays. Point mutations in the PH domain of the myo1e tail construct in pEGFP-C1 vector were introduced using the QuickChange II mutagenesis kit (Stratagene). The K772A mutant was generated using primers 5′-gcagacacagtcaccgcgtatgacaggagg-3′ and 5′-cctcctgtcatacgcggtgactgtgtctgc-3′. The R782A mutant was generated using primers 5′-caagggtgtaaaggcagacctgctccttacc-3′ and 5′-ggtaaggagcaggtctgcctttacacccttg-3′. Swiss 3T3 cells stably expressing DsRed-clathrin light chain were a generous gift of Dr. W. Almers, Vollum Institute, Oregon Health and Science University. Swiss 3T3 cells were maintained in DMEM/10% FBS in the presence of 0.5 mg/mL G-418. Cells were plated in 35 mm glass-bottom dishes (MatTek, Ashland, MA) and transfected with EGFP-myo1e constructs using 1 μg of DNA and 3 μL of lipofectamine 2000 (Invitrogen) 1 day prior to imaging. TIRF images of live cells were collected using a Nikon Eclipse TE2000-E multimode TIRF microscope equipped with a 60×, NA 1.45 TIRF Plan Apo objective. During imaging, cells were maintained in DMEM with 25 mM HEPES, pH 7.4, and 5% FBS at 37 °C. Colocalization of fluorescent puncta in red and green channels was analyzed manually using ImageJ. Individual fluorescent spots were independently identified in the red and green channels, and red clathrin puncta that were either positive or negative for myo1e were counted to determine percent colocalization. At least three dishes of cells transfected and imaged on different dates were analyzed for each construct.

RESULTS

Myo1e Tail Binds Phosphoinositides and Phosphatidylserine Tightly. We determined the effective dissociation constants (K_{eff}) of GFP-myo1e tail binding to LUVs containing 2% phosphoinositides and 98% DOPC by sedimentation assays. GFP-myo1e tail was mixed with sucrose-loaded LUVs containing PtdIns(4,5)P_2, PtdIns(3,5)P_2, or PtdIns(3,4,5)P_3 with synthetic 18:1 acyl chains or natural PtdIns(4,5)P_2 (mixed acyl chains) and centrifuged to separate the bound and the unbound protein. Unbound protein was measured as GFP fluorescence in the supernatant. Plots of fraction bound versus total lipid concentration were fit to hyperbolas to obtain K_{eff} (Figure 2, Table 1). No binding was observed between GFP-myo1e tail and LUVs composed of 100% DOPC or between GFP-His_6 and LUVs composed of 2% PtdIns(4,5)P_2 or 80% DOPS (Figure 2).

GFP-myo1e tail bound tightly to all of the phosphoinositides tested with slightly higher affinity for PtdIns(4,5)P_2 and PtdIns(3,4,5)P_3 over PtdIns(3,5)P_2 (Table 1). The K_{eff} for mixed acyl-chain 2% PtdIns(4,5)P_2 was 5.5 ± 0.49 μM, while the K_{eff} for 2% PtdIns(4,5)P_2 with a synthetic 18:1 acyl chain was 3.6 ± 0.60 μM. GFP-myo1e tail bound equally well to PtdIns(4,5)P_2 and PtdIns(3,4,5)P_3 (K_{eff} = 3.4 ± 0.52 μM), indicating that myo1e does not distinguish between these two phosphoinositides. Binding of GFP-myo1e tail to PtdIns(3,5)P_2 was more than 2-fold weaker (K_{eff} = 9.0 ± 2.4 μM) than binding to PtdIns(4,5)P_2 or PtdIns(3,4,5)P_3. Magnesium (1 mM) weakened binding to PtdIns(4.5)P_2 less than 1.5-fold (Table 1).

GFP-myo1e tail binds to LUVs containing 20% DOPS with a K_{eff} of 14 ± 2.3 μM, which is weaker than myo1e binding to 2% PtdIns(4,5)P_2, despite the higher negative charge in the 20% DOPS LUVs. The affinity of GFP-myo1e for 20% DOPS + 2% PtdIns(4,5)P_2 (mixed acyl chain) was ~3-fold higher than in the absence of DOPS. The affinity of GFP-myo1e tail for 80% DOPS was substantially higher (K_{eff} = 0.48 ± 0.092 μM) than for phosphoinositide-containing LUVs.

We determined the effective dissociation constant in terms of the accessible negative charge by measuring GFP-myo1e tail binding to LUVs containing a range of (0.5−8%) PtdIns(4,5)P_2 and (2%, 80%) DOPS mole percentages. A plot of the fraction of GFP-myo1e tail bound versus concentration of accessible negative charge shows that the affinities of the various LUVs are similar when normalized to charge (Figure 3a). However, in the presence of 20% DOPS, the normalized plots show weaker

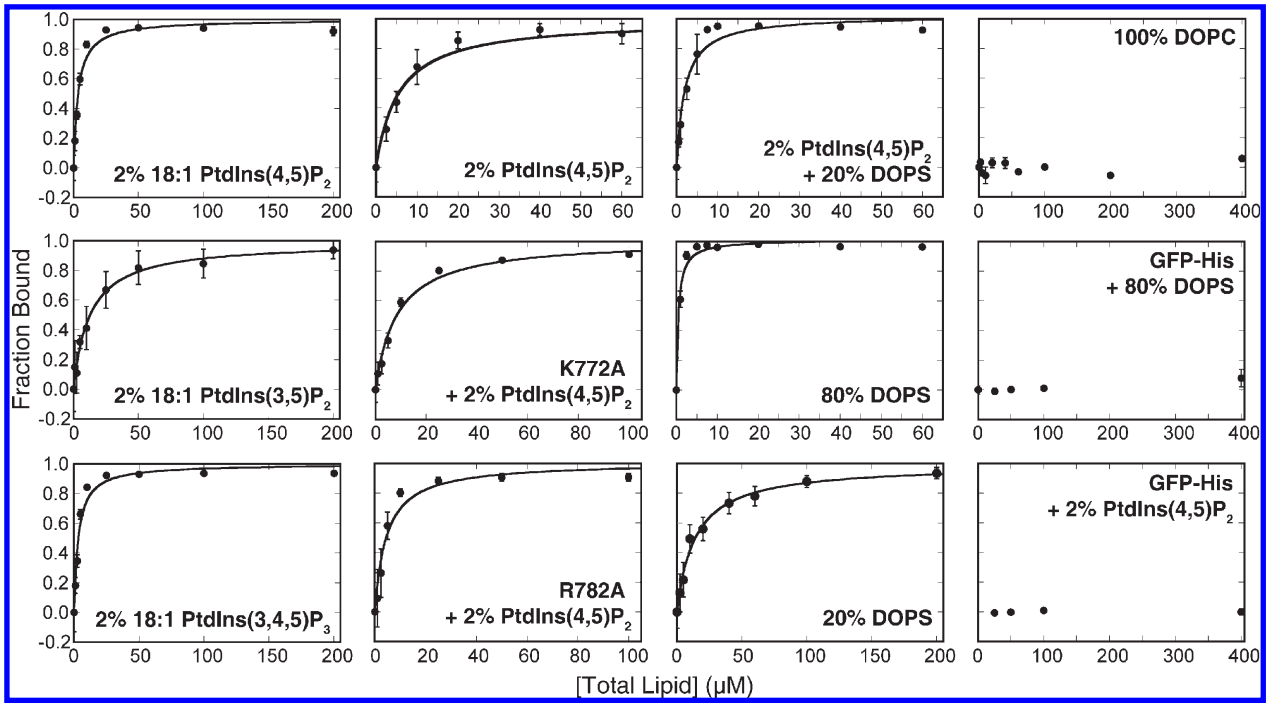

FIGURE 2: Binding of the myo1e tail to LUVs. Fraction of bound GFP-myo1e tail (40 nM total concentration), as measured by sedimentation assays, is plotted as a function of total lipid concentration. Each point is the average of 2−12 measurements. Error bars show standard deviations. The solid lines are the best fits of the data to a hyperbola. The K_{eff}^{lipid} for each data set is listed in Table 1 or Table 2.

Table 1: Effective Dissociation Constants (K_{eff}^{lipid}) for 40 nM GFP-Myo1e Tail Binding to LUVs As Measured in Sedimentation or Fluorescence-Quenching Assays

	K_{eff}^{lipid} (μM)			
LUV composition	GFP-myo1e-tail WT sedimentation	GFP-myo1e-tail WT fluorescence quenching	GFP-myo1c-tail sedimentation	myo1c-tail[a] sedimentation
2% mixed-chain PtdIns(4,5)P_2	5.5 ± 0.49 (6)[b]	3.6 ± 0.66 (3)	18 ± 4.6 (2)	23 ± 5.0
2% mixed-chain PtdIns(4,5)P_2 + 1 mM Mg^{2+}	ND	4.9 ± 0.61 (1)	ND	ND
2% 18:1 PtdIns(4,5)P_2	3.5 ± 0.34 (2)	1.3 ± 0.32 (2)	ND	ND
2% 18:1 PtdIns(3,5)P_2	13 ± 2.1 (3)	4.6 ± 0.81 (2)	ND	ND
2% 18:1 PtdIns(3,4,5)P_3	3.2 ± 0.40 (2)	1.2 ± 0.31 (2)	ND	ND
2% PtdIns(4,5)P_2 + 20% DOPS	1.9 ± 0.21 (4)	ND	4.9 ± 0.77 (2)	4.0 ± 1.5
20% DOPS	14 ± 2.3 (2)	ND	>400 (2)	>400
80% DOPS	0.51 ± 0.10 (2)	1.1 ± 0.23 (3)	1.2 ± 0.13 (2)	4.1 ± 0.70
100% DOPC	>400	>400	>400	>400

[a]Values from ref 5. [b]Errors report the standard error of the fit. Numbers in parentheses indicate the number of averaged experiments.

binding. This result is similar to what has been found for *Acanthamoeba* myosin-IC and suggests that binding depends on charge density in the membrane, as shown for vertebrate myo1c (*23*, *24*).

We note that the LUVs used in these binding studies are composed of simplified lipid mixtures and do not fully reflect the complexity of the plasma membrane. Additional anionic lipid species, such as phosphatidylinositol, or higher concentrations of phosphoinositides or phosphatidylserine could enhance myo1e binding, while lower concentrations of anionic lipids would reduce myo1e binding. Lipid composition varies significantly between cell types and cellular compartments (*25*), so it is difficult to replicate cellular membranes using defined lipid mixtures. Despite these shortcomings, our assays show that myo1e binds tightly to low concentrations of anionic lipids (0.5% PtdIns(4,5)P_2 or 20% DOPS), suggesting that the interactions measured here are physiologically significant.

Signature Residues in the Putative Myo1e PH Domain Are Not Required for in Vitro or in Vivo Membrane Binding. We performed binding experiments with GFP-myo1e-tail proteins containing alanine mutations at conserved PH domain residues (K772A and R782A; Figure 1) and found that the mutants have affinities for PtdIns(4,5)P_2 that are similar to the wild-type protein (Table 2; Figure 2). The K_{eff} for the R782A mutant (4.5 ± 1.2 μM) was the same as that for wild type, while the K_{eff} for the K772A mutant (8.5 ± 1.0 μM) was less than 2-fold weaker than that of wild type (Figure 2).

We examined the localization of GFP-myo1e-tail PH domain mutants in Swiss 3T3 cells expressing DsRed-tagged clathrin light chain using TIRF microscopy. Earlier studies showed that either deletion of the TH1 domain or a mutation in the SH3 domain reduced colocalization of myo1e with clathrin, suggesting that interactions with both lipids and proteins contribute to myo1e localization *in vivo* (*17*). As previously described (*17*), wild-type myo1e tail, similarly to the full-length myo1e, colocalizes with DsRed-clathrin-containing puncta at the plasma membrane. Like wild-type myo1e tail, both the K772A and R782A mutants colocalize with punctate regions of clathrin at the cell membrane,

which are presumably sites of endocytosis (Figure 4). These results are in contrast to experiments using myo1c proteins with homologous mutations that do not bind to phosphoinositides in sedimentation assays or to cellular membranes in live cells (*9*, *12*, *13*).

Soluble Inositol Phosphates Do Not Efficiently Compete with Phosphoinositides for Myo1e Binding. High concentrations (>100 μM) of soluble Ins(1,4,5)P_3 are required to completely dissociate 40 nM GFP-myo1e tail from 10 μM 2% PtdIns(4,5)P_2 LUVs (Figure 3b), indicating that InsP(1,4,5)P_3 does not equivalently compete with PtdIns(4,5)P_2 in LUVs for GFP-myo1e-tail binding. However, it is of note that Ins(1,4,5)P_3 induces dissociation, as this effect does not appear to be simply due to the addition of soluble, clustered negative charge, since 50−500 μM ATP does not dissociate GFP-myo1e tail from membranes (not shown). Assuming stoichiometric and competitive binding (which is likely an oversimplification), the effective affinity of Ins(1,4,5)P_3 for GFP-myo1e tail is 11 ± 2.0 μM (Figure 3b). This weak affinity of GFP-myo1e tail for Ins(1,4,5)P_3 is in contrast to similar experiments performed with myo1c tail, which binds Ins(1,4,5)P_3 with an effective affinity of 96 ± 32 nM (*9*).

Binding of GFP-Myo1e Tail to LUVs Is Fast. The fluorescence of GFP-myo1e tail decreases when mixed with LUVs containing anionic phospholipids. This quenching linearly

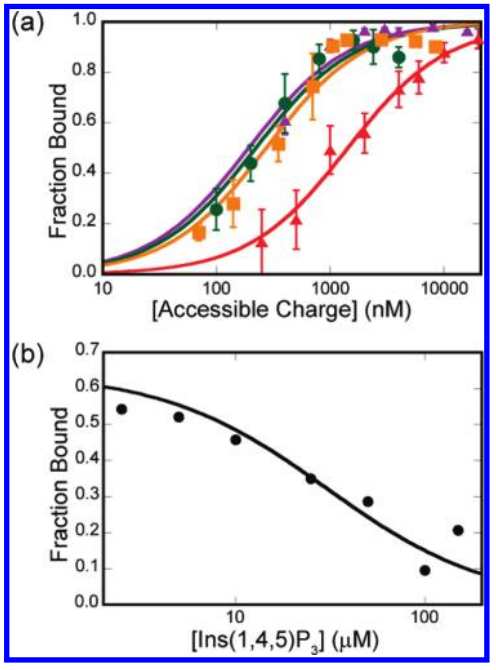

FIGURE 3: Binding of 40 nM GFP-myo1e tail to lipids. (a) Fraction of bound GFP-myo1e tail, as determined by sedimentation assays, is plotted as a function of accessible negative charge. Binding curves for LUVs containing 2% PtdIns(4,5)P_2 (green), 20% DOPS (red), 80% DOPS (violet), or 2% PtdIns(4,5)P_2 + 20% DOPS (orange) were fit to a quadratic equation in Experimental Procedures. Error bars indicate standard deviation. (b) Binding of 40 nM GFP-myo1e tail to LUVs containing 2% PtdIns(4,5)P_2, as determined by stopped-flow fluorescence quenching experiments, at a total lipid concentration of 10 μM in the presence of 2.5−200 μM Ins(1,4,5)P_3. The solid line is the best fit to the data using the competition binding equation previously described (*9*). The effective dissociation constant obtained from this fit is 11 ± 2.0 μM.

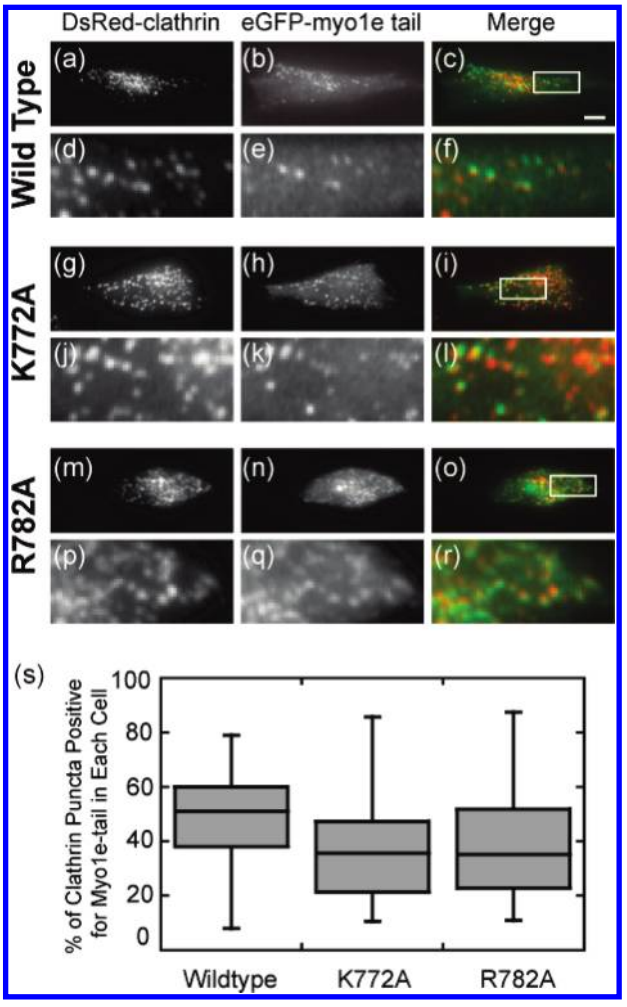

FIGURE 4: *In vivo* localization of eGFP-myo1e-tail wild type and PH domain mutants in Swiss 3T3 cells. (a−r) Localization of DsRed-tagged clathrin (a, d, g, j, m, p) and eGFP-tagged wild-type (b, e) or mutant (h, k, n, q) myo1e-tail constructs as observed by TIRF microscopy. Merged images are shown in panels c, f, i, l, o, and r. The boxed regions in panels c, i, and o are shown at a higher magnification in panels d−f, j−l, and p−r, respectively. Bar, 10 μm. (s) Analysis of colocalization of Myo1e-tail puncta with clathrin puncta. % of clathrin puncta in each cell that was also positive for Myo1e tail was determined as described in Experimental Procedures. Numbers obtained for individual cells are plotted as a box-and-whisker plot, with the horizontal line representing the median, boxes representing the second and third quartiles, and whiskers indicating the bottom and top quartiles. Total number of clathrin puncta counted was 1304 in 32 cells expressing wid-type tail, 754 in 28 cells expressing K772A mutant, and 834 in 35 cells expressing R782A mutant.

Table 2: Effective Dissociation Constants (K_{eff}^{lipid}) for GFP-Myo1e-Tail Wild Type and PH Domain Mutants Binding to 2% PtdIns(4,5)P_2 LUVs As Measured in Sedimentation Assays

	K_{eff}^{lipid} (μM)		
LUV composition	GFP-myo1e-tail WT	GFP-myo1e-tail K772A	GFP-myo1e-tail R782A
2% mixed-chain PtdIns(4,5)P_2	5.5 ± 0.49 (6)[a]	8.5 ± 1.0 (2)	4.5 ± 1.2 (2)

[a]Errors report the standard error of the fit. Numbers in parentheses indicate the number of averaged experiments.

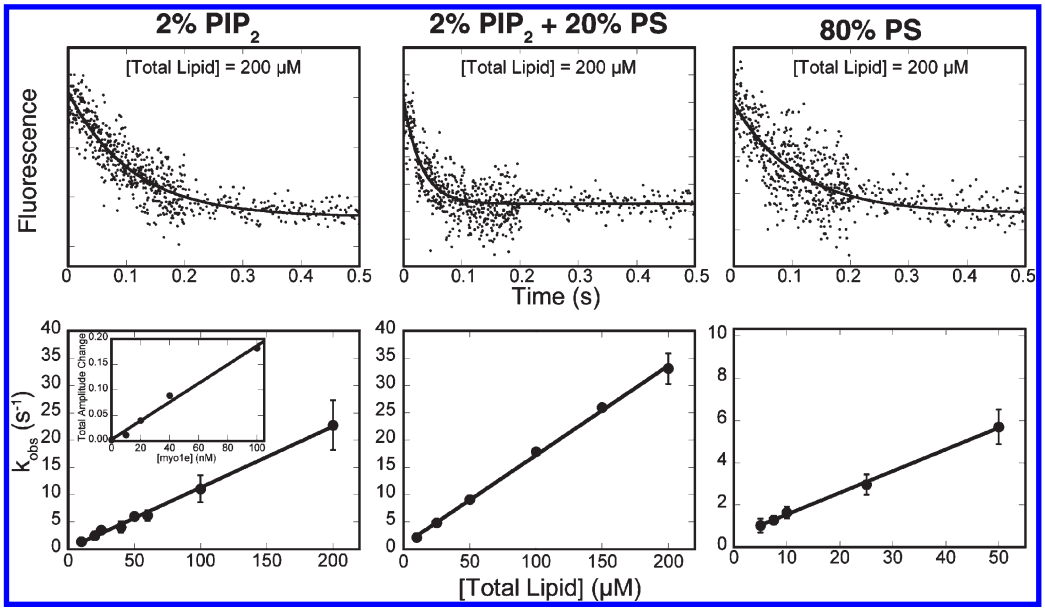

FIGURE 5: Association of myo1e tail with LUVs. Myo1e tail was rapidly mixed with LUVs containing DOPC with 2% PtdIns(4,5)P_2, 2% PtdIns(4,5)P_2 + 20% DOPS, or 80% DOPS. (Top) Fluorescence decreases as a function of time. Final concentrations are 40 nM GFP-myo1e tail and 200 μM total lipid. Solid lines are the best fits of data to a single-exponential function. (Bottom) The rates of k_{fast} are plotted as a function of total lipid concentration. Each data point represents the average of two to four experiments. Error bars indicate standard deviation. The solid lines are the best linear fit to the data. $k_{association}$ and y-intercept values determined from these plots are reported in Table 3. (Bottom inset) Fluorescence amplitude change upon addition of PtdIns(4,5)P_2 LUVs is linearly related to GFP-myo1e-tail concentration. LUVs composed of 2% PtdIns(4,5)P_2 at a concentration of 100 μM total lipid were rapidly mixed with increasing concentrations of GFP-myo1e tail (0−100 nM after mixing). Transients were fit to a single- or double-exponential function as described in Experimental Procedures, and the amplitudes of the transient fluorescent changes are plotted as a function of the GFP-myo1e-tail concentration. The solid line represents a linear fit to the data.

reports the concentration of GFP-myo1e tail bound to LUVs, as the amplitude change on addition to 100 μM 2% PtdIns(4,5)P_2 is linearly related to protein concentrations in the range of 20−100 nM GFP-myo1e tail (Figure 5, inset). Changes in fluorescence were not observed when GFP-myo1e tail was mixed with 100% DOPC LUVs or when GFP alone was mixed with 2% PtdIns-(4,5)P_2 LUVs (data not shown). Additionally, steady-state affinities (K^{eff}_{lipid}) determined from fluorescence quenching are similar to those determined by sedimentation assays (Table 1). Therefore, we used this fluorescence change to measure the rate of GFP-myo1e-tail binding to LUVs in stopped-flow fluorescence experiments.

Fluorescence time courses were fit with exponential functions, as described in Experimental Procedures. The rate of fluorescence quenching (k_{fast}) increased linearly with the lipid concentration from 5 to 200 μM (Figure 5). In some experiments, a slow phase (k_{slow}) was present in the fluorescence transients (< 30% of the amplitude). This variable slow component was not considered in our analyses.

The apparent second-order rate constant (k_a) for binding of GFP-myo1e tail to LUVs was determined by plotting k_{fast} as a function of total lipid concentration (Figure 5) for each LUV composition. Association rate constants obtained from linear fits to the data, in terms of total lipid concentration, are provided in Table 3. The association rate constants are near the diffusion limit when calculated in terms of LUV concentration, similar to those measured for myo1c binding to LUVs of similar composition (*24*). GFP-myo1e-tail dissociation rates were calculated as the product of equilibrium dissociation constants and association rate constants ($k_{dis} = K_{eff}k_a$; Table 3). The rate of dissociation from LUVs containing 2% PtdIns(4,5)P_2 and 20% DOPS (0.15 s^{-1}) is 8-fold slower than the actin-activated steady-state myo1e ATPase rate (1.2 s^{-1}) (*26*), indicating that myo1e could remain attached to the membrane for multiple ATPase cycles.

Table 3: Association and Dissociation Kinetics of GFP-Myo1e Binding to LUVs

LUV composition	k_a ($\times 10^5$ M^{-1} s^{-1})	y-intercept (s^{-1})	calc k_{diss} (s^{-1})
2% PtdIns(4,5)P_2	1.1 ± 0.080 (3)[a]	0.13 ± 0.74	0.40
2% PtdIns(4,5)P_2 + 20% DOPS	1.6 ± 0.051 (3)	0.83 ± 0.49	0.15
80% DOPS	1.0 ± 0.086 (3)	0.53 ± 0.20	0.058

[a]Errors indicate the standard error of the fit. Numbers in parentheses indicate the number of averaged experiments.

DISCUSSION

Our results demonstrate that GFP-myo1e tail binds with high affinity to low concentrations of DOPS or phosphoinositides, and tight membrane binding does not require the conserved basic residues of the phosphoinositide-binding region in the $\beta 1/\beta 2$ loop of the PH domain (Figure 2). The accessible negative charge of the membrane appears to be the crucial determinant of *in vitro* membrane affinity (Figure 3b), with only a minor contribution from a stereospecific protein−phosphoinositide interaction. These membrane binding properties are similar to those found for *Acanthamoeba* myosin-IC (*8*).

The location of the myo1e membrane binding site is not known, and based on investigations of other isoforms, it is likely to be distributed throughout the tail. The putative PH domain has been shown to be important for membrane binding in some isoforms (*9*, *12*−*14*), as are flanking regions, termed pre-PH and post-PH, that have been shown to play a role in the *in vivo* localization of myo1g (*12*). Additionally, the regulatory domains of myo1a and myo1c have been

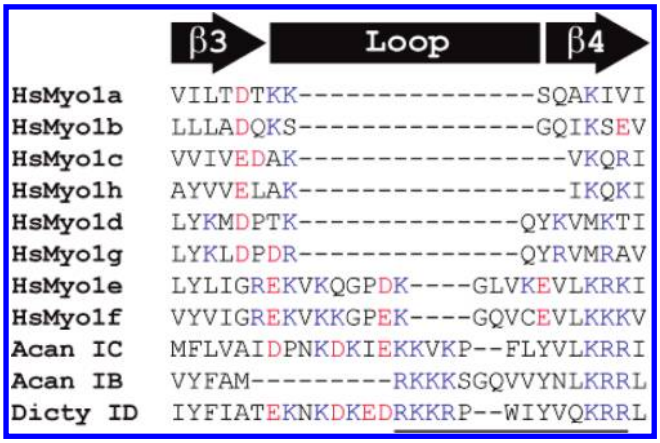

FIGURE 6: Sequence alignment of the $\beta3/\beta4$ region of myosin-1 PH domains. Blue indicates basic residues, and red indicates acidic residues. The line at the bottom of the alignment marks the peptide used in Brzeska et al. (*8*).

proposed to play roles in direct lipid binding and subcellular targeting (*5*, *9*, *12*, *27*, *28*).

Two previous studies offer insight into which regions of the myo1e tail might mediate electrostatic interactions with lipids. Brezska et al. (*29*) developed a sequence analysis algorithm (BH-Search) to identify regions with basic and hydrophobic residues that could interact with acidic lipids. Running the BH-Search algorithm on the myo1e tail identifies a region flanking the $\beta1/\beta2$ loop of the myo1e PH domain as a potential lipid interaction site (Supporting Information Figure S1). The $\beta1/\beta2$ loop is part of the PH domain signature motif and is flanked by the conserved lysine and arginine residues that were mutated in this study, but the BH-Search results suggest that the mutants tested in our binding assays would retain their lipid binding capability. In a separate study, Brzeska et al. (*8*) identified the $\beta3/\beta4$ loop of the putative PH domain in *Acanthamoeba* myosin-IC as a potential membrane binding site (Figure 6). A synthetic peptide of this sequence, which primarily consists of basic and hydrophobic residues that are conserved in myo1e, but not myo1c and other short-tailed myosins, effectively competes with *Acanthamoeba* myosin-IC for membrane binding. The BH-Search algorithm did not identify the homologous region within myo1e, likely because of the presence of acidic residues in the $\beta3/\beta4$ loop (Figure 6). However, the increased size and basic character of this region is conserved in myo1e, so its role in membrane binding cannot be ruled out. High-resolution structural characterization of myosin-I tail domains will likely be required to obtain a complete understanding of this interaction.

We previously proposed that myo1c, a short-tailed isoform, binds to membranes via two sites, a PH-domain-mediated phosphoinositide-specific site that is crucial for membrane binding and a secondary binding site that binds negatively charged phospholipids via electrostatic interactions (*24*). The current study shows that myo1e binds lipids by a distinct mechanism. The primary myo1e lipid binding site likely binds with high affinity via electrostatic interactions, as binding requires neither phosphoinositides nor the PH domain signature residues. However, a high concentration of soluble Ins(1,4,5)P_3 is able to compete with LUVs for GFP-myo1e-tail binding (Figure 3b), suggesting that myo1e has a region with phosphoinositide specificity. Binding to PtdIns(3,5)P_2 was more than 2-fold weaker than binding to either PtdIns(4,5)P_2 or PtdIns(3,4,5)P_3, indicating that myo1e has some stereospecificity for phosphoinositides with a phosphate at the 4-position of the inositol ring, likely mediated by low-affinity binding via the PH domain. On the basis of these results, we propose that myo1e binds to membranes via two sites, a primary binding site with high-affinity electrostatic interactions and a second low-affinity phosphoinositide-specific site, likely the PH domain. Myo1e may remain tightly attached to the membrane via the nonspecific binding, as we proposed for myo1c, and phosphoinositides may be able to associate and dissociate from the PH domain while myo1e remains attached to the membrane.

The direct binding of myo1e to negatively charged lipids suggests several possible mechanisms by which myo1e could function at the plasma membrane. Myo1e, anchored by lipid interactions, could concentrate myo1e-binding proteins, such as dynamin and synaptojanin-1, at actin-rich regions of the membrane. Conversely, myo1e-binding proteins could recruit myo1e to specific membrane regions, such as clathrin-coated pits, where myo1e might modulate phosphoinositide concentration. It is also possible that direct lipid binding provides additional mechanical strength to membrane interactions during active force production. Clearly, there is much to be learned about the molecular role of myo1e in membrane mechanics.

SUPPORTING INFORMATION AVAILABLE

One figure showing a plot of BH-Search results for the myo1e tail. This material is available free of charge via the Internet at http://pubs.acs.org.

REFERENCES

1. Zot, H. G., Doberstein, S. K., and Pollard, T. D. (1992) Myosin-I moves actin filaments on a phospholipid substrate: implications for membrane targeting. *J. Cell Biol. 116*, 367–376.
2. Nambiar, R., McConnell, R. E., and Tyska, M. J. (2009) Control of cell membrane tension by myosin-I. *Proc. Natl. Acad. Sci. U.S.A. 106*, 11972–11977.
3. Horowitz, J. A., and Hammer, J. A., III (1990) A new *Acanthamoeba* myosin heavy chain. Cloning of the gene and immunological identification of the polypeptide. *J. Biol. Chem. 265*, 20646–20652.
4. Adams, R. J., and Pollard, T. D. (1989) Binding of myosin I to membrane lipids. *Nature 340*, 565–568.
5. Swanljung-Collins, H., and Collins, J. H. (1992) Phosphorylation of brush border myosin I by protein kinase C is regulated by Ca(2+)-stimulated binding of myosin I to phosphatidylserine concerted with calmodulin dissociation. *J. Biol. Chem. 267*, 3445–3454.
6. Zot, H. G. (1995) Phospholipid membrane-associated brush border myosin-I activity. *Cell Motil. Cytoskeleton 30*, 26–37.
7. Hokanson, D. E., and Ostap, E. M. (2006) Myo1c binds tightly and specifically to phosphatidylinositol 4,5-bisphosphate and inositol 1,4,5-trisphosphate. *Proc. Natl. Acad. Sci. U.S.A. 103*, 3118–3123.
8. Brzeska, H., Hwang, K. J., and Korn, E. D. (2008) Acanthamoeba myosin IC colocalizes with phosphatidylinositol 4,5-bisphosphate at the plasma membrane due to the high concentration of negative charge. *J. Biol. Chem. 283*, 32014–32023.
9. Hokanson, D. E., Laakso, J. M., Lin, T., Sept, D., and Ostap, E. M. (2006) Myo1c binds phosphoinositides through a putative pleckstrin homology domain. *Mol. Biol. Cell 17*, 4856–4865.
10. Santy, L. C., Frank, S. R., Hatfield, J. C., and Casanova, J. E. (1999) Regulation of ARNO nucleotide exchange by a PH domain electrostatic switch. *Curr. Biol. 9*, 1173–1176.
11. Corbin, J. A., Dirkx, R. A., and Falke, J. J. (2004) GRP1 pleckstrin homology domain: activation parameters and novel search mechanism for rare target lipid. *Biochemistry 43*, 16161–16173.
12. Patino-Lopez, G., Aravind, L., Dong, X., Kruhlak, M. J., Ostap, E. M., and Shaw, S. (2010) Myosin 1G is an abundant class I myosin in lymphocytes whose localization at the plasma membrane depends on its ancient divergent pleckstrin homology (PH) domain (Myo1PH). *J. Biol. Chem. 285*, 8675–8686.
13. Olety, B., Walte, M., Honnert, U., Schillers, H., and Bahler, M. (2010) Myosin 1G (Myo1G) is a haematopoietic specific myosin that localises to the plasma membrane and regulates cell elasticity. *FEBS Lett. 584*, 493–499.

14. Komaba, S., and Coluccio, L. M. (2010) Localization of myosin 1b to actin protrusions requires phosphoinositide binding, *J. Biol. Chem.* (in press).
15. Swanson, J. A., Johnson, M. T., Beningo, K., Post, P., Mooseker, M., and Araki, N. (1999) A contractile activity that closes phagosomes in macrophages. *J. Cell Sci. 112* (Part 3), 307–316.
16. Stoffler, H. E., Ruppert, C., Reinhard, J., and Bahler, M. (1995) A novel mammalian myosin I from rat with an SH3 domain localizes to Con A-inducible, F-actin-rich structures at cell-cell contacts. *J. Cell Biol. 129*, 819–830.
17. Krendel, M., Osterweil, E. K., and Mooseker, M. S. (2007) Myosin 1E interacts with synaptojanin-1 and dynamin and is involved in endocytosis. *FEBS Lett. 581*, 644–650.
18. Krendel, M., Kim, S. V., Willinger, T., Wang, T., Kashgarian, M., Flavell, R. A., and Mooseker, M. S. (2009) Disruption of myosin 1e promotes podocyte injury. *J. Am. Soc. Nephrol. 20*, 86–94.
19. Liang, Y., Niederstrasser, H., Edwards, M., Jackson, C. E., and Cooper, J. A. (2009) Distinct roles for CARMIL isoforms in cell migration. *Mol. Biol. Cell 20*, 5290–5305.
20. Xu, P., Mitchelhill, K. I., Kobe, B., Kemp, B. E., and Zot, H. G. (1997) The myosin-I-binding protein Acan125 binds the SH3 domain and belongs to the superfamily of leucine-rich repeat proteins. *Proc. Natl. Acad. Sci. U.S.A. 94*, 3685–3690.
21. Putkey, J. A., Slaughter, G. R., and Means, A. R. (1985) Bacterial expression and characterization of proteins derived from the chicken calmodulin cDNA and a calmodulin processed gene. *J. Biol. Chem. 260*, 4704–4712.
22. Peitzsch, R. M., and McLaughlin, S. (1993) Binding of acylated peptides and fatty acids to phospholipid vesicles: pertinence to myristoylated proteins. *Biochemistry 32*, 10436–10443.
23. Tang, N., Lin, T., and Ostap, E. M. (2002) Dynamics of myo1c (myosin-ibeta) lipid binding and dissociation. *J. Biol. Chem. 277*, 42763–42768.
24. McKenna, J. M., and Ostap, E. M. (2009) Kinetics of the interaction of myo1c with phosphoinositides. *J. Biol. Chem. 284*, 28650–28659.
25. Vance, D. E., and Vance, J. E. (2008) Biochemistry of lipids, lipoproteins and membranes, 5th ed., Elsevier, Amsterdam and Boston.
26. El Mezgueldi, M., Tang, N., Rosenfeld, S. S., and Ostap, E. M. (2002) The kinetic mechanism of Myo1e (human myosin-IC). *J. Biol. Chem. 277*, 21514–21521.
27. Hirono, M., Denis, C. S., Richardson, G. P., and Gillespie, P. G. (2004) Hair cells require phosphatidylinositol 4,5-bisphosphate for mechanical transduction and adaptation. *Neuron 44*, 309–320.
28. Cyr, J. L., Dumont, R. A., and Gillespie, P. G. (2002) Myosin-1c interacts with hair-cell receptors through its calmodulin-binding IQ domains. *J. Neurosci. 22*, 2487–2495.
29. Brzeska, H., Guag, J., Remmert, K., Chacko, S., and Korn, E. D. (2010) An experimentally based computer search identifies unstructured membrane-binding sites in proteins: application to class I myosins, PAKS, and CARMIL. *J. Biol. Chem. 285*, 5738–5747.